A methodological framework for flood hazard assessment for land transport infrastructures

Published Version:
Samela, C., Carisi, F., Domeneghetti, A., Petruccelli, N., Castellarin, A., Iacobini, F., et al. (2023). A methodological framework for flood hazard assessment for land transport infrastructures. INTERNATIONAL JOURNAL OF DISASTER RISK REDUCTION, 85, 1-17 [10.1016/j.ijdrr.2022.103491].

Availability:
This version is available at: https://hdl.handle.net/11585/960888 since: 2024-02-23

Published:
DOI: http://doi.org/10.1016/j.ijdrr.2022.103491

A methodological framework for flood hazard assessment for land transport infrastructures

Caterina Samela[1*], Francesca Carisi[2], Alessio Domeneghetti[3], Natasha Petruccelli[3], Attilio Castellarin[3], Franco Iacobini[4], Alessandro Rinaldi[4], Alessandra Zammuto[4], Armando Brath[3]

[1] Institute of Methodologies for Environmental Analysis (IMAA), National Research Council (CNR), Tito Scalo (Potenza), Italy.

[2] Interregional Agency for the Po river (AIPO), Parma, Italy.

[3] Department of Civil, Chemical, Environmental and Materials Engineering (DICAM), University of Bologna, Bologna, Italy.

[4] Technical Department, Rete Ferroviaria Italiana (RFI) S.p.a., Rome, Italy.

[*]Corresponding author: Caterina Samela, caterina.samela@imaa.cnr.it

Abstract

The complexity of land transport infrastructures, their length and the heterogeneity of potential hazardous scenarios across large areas make flood hazard assessment a challenging task. We propose a parsimonious, rapid and operational procedure that enables large scale applications and, at the same time, a detailed evaluation of individual segments of linear transport infrastructures. In particular, we focus on extensive land transport infrastructure networks (i.e., railways) and propose a methodological framework for: (1) identifying segments of the network that are prone to fluvial flooding, and (2) grouping the identified elements into different hazard classes depending on the mechanism and severity of the expected flooding scenario (i.e., damage due to potential embankment overtopping, embankment instability due to infiltration, erosion or washout, train or vehicles collision against fluvial deposits or debris, etc.). Network sections at risk, as well as main hazardous flood indices (e.g., water depth), are estimated referring to official inundation maps, when available, or by means of Digital Elevation Model (DEM)-based algorithms and geomorphic indices (e.g., Geomorphic Flood Index-GFI). In addition, a DEM-based approach is proposed to identify potential debris flow sources threatening the infrastructure. The procedure has been developed and tested for the Italian Railway Network (focusing on seven river basins), but it can be adapted to different cases and different land transport infrastructures. A first comparison with historical flood events proves the potential of the procedure, which can support stakeholders in planning measures for managing and mitigating the flood risk associated with the transport networks across large spatial scales.

Keywords: transport infrastructures; railway systems; flood hazard; debris-flow; DEM-based approach; Geomorphic Flood Index.

1. Introduction

A reliable transport infrastructure is one of the cornerstones of a thriving economy due to its fundamental role in economic and social development. Industrialized countries are generally characterized by transport infrastructure networks (e.g. roads and railways) significantly extended. As such, they are exposed to a variety of adverse meteoric and hydrogeological events (e.g. intense rainfall, floods, erosion, landslides, etc.) (Petrova & Bostenaru, 2020). These phenomena can produce a series of negative impacts on linear transport infrastructures, including accidents, damages to the infrastructures and/or their components, delays, interruptions and malfunctions, causing significant direct and indirect socio-economic losses (Nester et al., 2008; Moran et al., 2010; Kellermann et al., 2015; Jaroszweski et al., 2010; Otto et al., 2019). Even a damage of a single infrastructure element/segment can lead to a systemic loss of connection and efficiency of the transport network, generating socio-economic losses in the short and long term.

The present work focuses on hazards related to flood phenomena, which in the period 2000 to 2019 represented the most common type of disaster worldwide and, after storms, the costliest in terms of recorded economic damage (651 billion US$) (UNDRR, 2020).

Examples are the extensive damages to infrastructures occurred during Hurricane Maria in Puerto Rico in 2017, and those caused by the Tbilisi (Georgia) floods in June 2015, where the cost of transport assets represented approximately 60% of the total damage (Koks et al., 2019). Another example is the severe damage suffered by the Austrian Federal Railways due to floods events occurred in central Europe in May and June 2013, which affected track structures, caused widespread service disruptions, with a total cost of about 84 million USD (Kellermann et al., 2016). These numbers give confidence that flooding can be catastrophic for transportation networks and their users. In addition, the expected damage due to flood phenomena is destined to rise in future decades as a consequence of the economic and social development in areas exposed to flood (Domeneghetti et al., 2015; Liu et al., 2020; Tellman et al., 2021) and because of the increase in the extent and socio-economic function of transport systems (Dawson et al., 2016). Also, ongoing climate change may play a role in increasing the frequency of flood events responsible for such damages (see, e.g. Hall et al., 2005; de Moel et al., 2011; Blöschl et al., 2019).

In this scenario, there is a clear need to design a methodological framework aimed at evaluating the flood-related hazard for extended transportation networks, paving the way for the identification of high-risk components and an effective maintenance and mitigation measures planning.

Tackling the flood-induced hazard assessment of land transport networks requires dealing with some specific issues that characterize such phenomena: i) major river floods are usually driven by large-scale atmospheric circulations, thereby affecting large areas (Prudhomme and Genevier, 2011; Lavers et al., 2013) with the potential of disrupting several network components concurrently (Zhu et al., 2021). Thus, methods allowing an assessment over large areas are essential. ii) Working at large spatial scales means considering infrastructure length and complexity, the computational issues of running large scale hydraulic models and the widespread lack of appropriate and detailed flood hazard data (Chang et al. 2010). As a consequence, several studies assessed natural hazards impacts on transportation infrastructures avoiding a detailed treatment at the asset level and preferring a system-level perspective (Chang et al., 2010; Gil and Steinbach, 2008; Kellermann et al., 2016; Lamb et al., 2019; Koks et al., 2019). For instance, Koks et al., (2019) performed an estimate of the global risk of road and railway assets extracted from OpenStreetMap (OSM) to different types of natural hazards, among which flooding, making use of state-of-the-art global hazard maps. They found that ~7.5% of the road and railway assets are exposed to a 1/100 years flood event and also that surface and river flooding presents the highest expected annual exposure levels in most countries (globally 39% and 34%, for surface and river flooding, respectively). In other works, the networks have been modelled with simplified approaches where a fixed percentage of damage to linear networks is estimated depending on the phenomenon of interest (Kellerman et al., 2016; Otto et al., 2019) or using generalized assumptions on infrastructure density rather than considering individual segments or bridge structures (Koks et al., 2019). More advanced approaches, although still rare, evaluate the interaction between the various phenomena and the infrastructure through, for example, fragility functions, statistical and empirical approaches, probabilistic analyses and machine-learning models (see e.g. Tsubaki et al., 2016; Guikema, 2009). In this sense, a significant example is the recent work by Van Ginkel et al. (2021), who performed a flood risk assessment for the European road network by adopting an object-based approach applied to high-resolution exposure data (Open Street Map), allowing to account for segment-specific attributes (i.e., individual road segments) and thus allowing for targeted risk reduction strategies. Some other approaches focused on the impacts of the transport network malfunction on society, such as those based on various economic theories and simulation techniques for the evaluation of the dynamic behavior of transport systems (see e.g. Perez- Morales et al., 2019; Dunn et al., 2013; Guze, 2014; Pregnolato et al., 2017). The majority of these works are conceived on a case-study basis, where historical scenarios were available (Hong et al., 2015), or investigated flood impacts on transportation systems focusing on the vulnerability of assets (Kellermann et al., 2015; Pregnolato et al., 2017; Singh et al., 2018; Koks et al., 2019). All these efforts attempt to develop tools capable to support transport infrastructure managers in ranking intervention priorities on the individual elements of the networks (Kellermann et al, 2015; 2016; Otto et al., 2019). However, the implementation of detailed investigations to large geographical areas is still limited.

In this context, we propose a parsimonious and operational approach that allows rapid large-scale implementation and, at the same time, a detailed treatment at the transport segment level. Among the various types of linear infrastructures, this work focuses on railway networks, although the methodology can be easily adapted to road and motorway networks.

The methodological and knowledge advances presented in this work originate from a collaboration with Rete Ferroviaria Italiana (RFI) S.p.A., the public body that manages the Italian railway infrastructure. The increasing awareness about flood hazard and the progress made in the knowledge of its spatial distribution on the Italian national territory (i.e., extensive flood hazard mapping in actuation of 2007/60/CE Flood Directive) offer the appropriate groundwork to investigate flood-related hazard for railway infrastructures. Referring to hazardous maps of the River Basin Authorities, out of a total of 16.787 km of Italian railway network, about 4000 km (nearly 24%) are exposed to flooding, erosion, etc., while nearly 2500 km belongs to areas prone to landslides, subsidence, mud flow, etc.. A recent investigation of Firmi et al. (2021) depicts an even more severe condition, highlighting that approximately 7700 km of railway network extend through hilly and mountainous areas potentially susceptible to landslides and 9000 km in urban floodplains potentially intersected by hydraulic phenomena. The uncertainty on hazard estimation stems from the fact that a significant portion of railway segments runs through areas were hydrogeological hazards is not properly investigated: detailed studies are resource intensive and thus limited to major rivers and more critical hydraulic nodes. This condition is frequent in both developed and developing countries.

The proposed approach aims at enhancing the assessment of flood-related hazards of physical transport infrastructures. In particular, innovative elements can be summarized as follows: i) high spatial resolution, since the approach looks at elementary segments of the railway network; ii) characterization of type and severity of expected flood phenomena for each segment (i.e., damage due to potential embankment overtopping, embankment instability due to infiltration, erosion or washout, train or vehicles collision against fluvial deposits or debris, etc.); iii) flood hazard classification, giving account of the intervention priority; iv) assessment of the hazard associated with the overall river network: the approach refers to pre-existing state-of-the-art flood hazard maps, but it also incorporates hydro-geomorphic fast-processing methods (e.g. the Geomorphic Flood Index, Samela et al., 2017; 2018) to extend the identification of flood- and debris-prone areas for territories lacking detailed investigations.

The proposed methodological structure has been developed with the perspective of large-scale application (i.e., national), where the identification and prioritization of intervention measures would enable stakeholders to implement appropriate risk-mitigation strategies and prepare effective network management plans under alert and emergency conditions, with the aim of promoting a proactive approach and prevent the adverse impacts of natural hazards. It this sense, it is worth mentioning that a quantitative estimation of severity, costs, impacts and disruption associated to a flood-related events is out of the scope of the current work. Nevertheless, the outcomes achievable by implementing the presented approach represent key information for future works aimed at advancing the risk assessment towards such targets.

2. Methods

The identification of infrastructures at risk and the classification of different flood phenomena threatening them is carried out following the workflow schematized in Figure 1. In particular, the methodological framework entails three sequential steps:

1) identification of the railway section (RS) potentially affected by water-related hazardous scenarios (i.e., adopting official hazard maps or other; see section 2.1);

2) characterization of the hazardous events based on few geomorphic parameters (e.g., slope, concentration time, debris flow triggering sources, etc.) estimated by analyzing the topography of the basin derived from a DEM (Digital Elevation Model);

3) identification of associated damage scenarios and flood hazard class attribution based on previously estimated parameters.

Criteria, assumptions and threshold values adopted for the implementation of the methodological framework are described and discussed in the following sections.

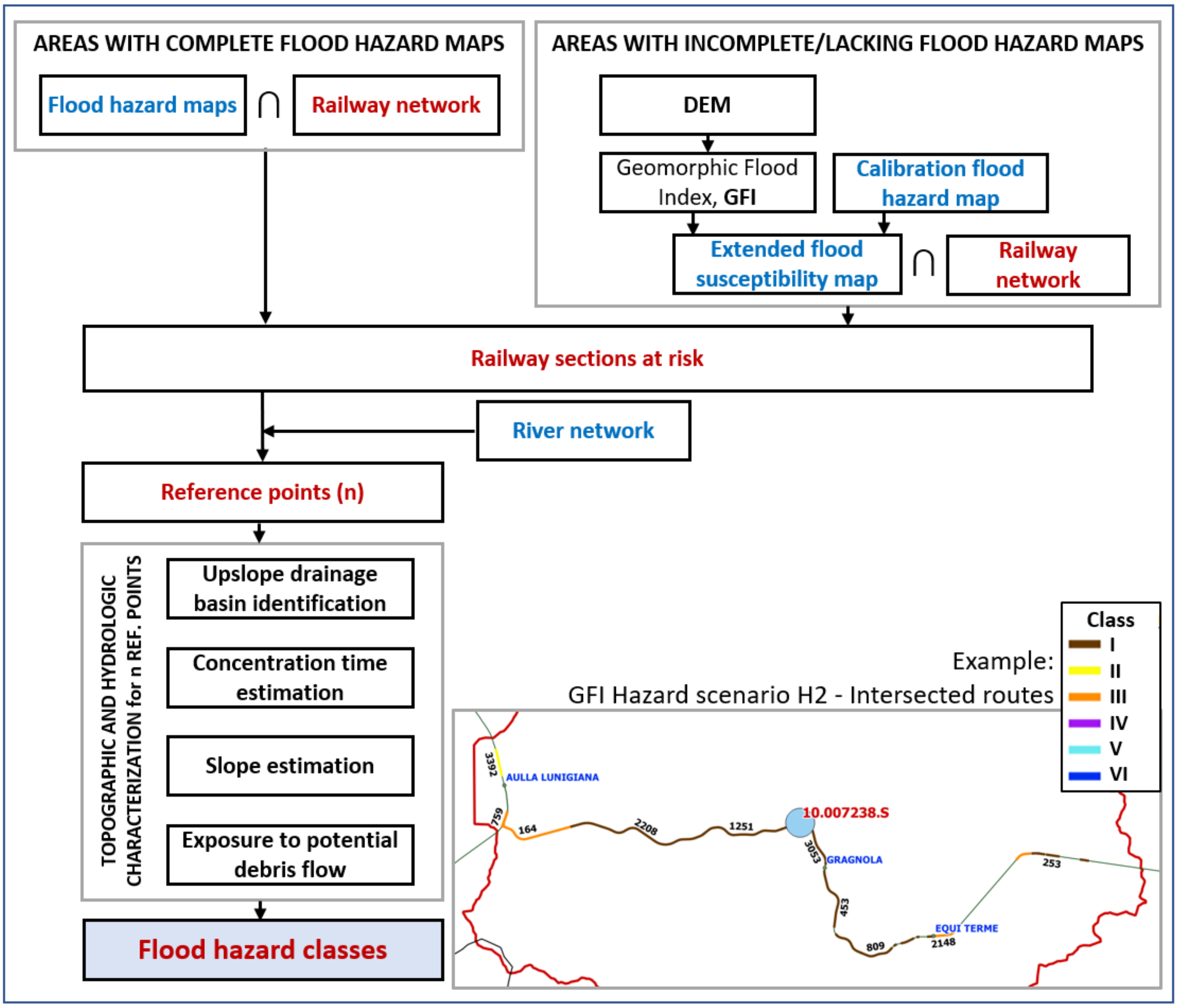

Figure 1. Workflow for the identification of the railway sections (RSs) affected by water-related hazardous scenarios and the consequent classification of flood phenomena.

2.1 Identification of flood-prone areas and affected railway

The proposed methodology affords this task distinguishing two common situations: i) areas for which flood inundation maps are available from the competent Authorities (e.g., the District Basin Authorities in Italy); this case is illustrated in section 2.1.1. ii) areas that, to date, have not been the object of detailed flood hazard assessments. Generally, this latter condition is more common for main-river tributaries and minor stream-networks, for which historical data and detailed hydraulic investigations are not available. Procedures to deal with these cases are illustrated in section 2.1.2.

2.1.1 *Areas mapped in the national Flood Risk Management Plans (FRMPs)*

In Europe, the Floods Directive 2007/60/EC demands the basin authorities to provide the delimitation of areas affected by flood events for three scenarios: H1, which describes rare events (return period, Tr, up to 500 years), hazard scenario H2 describing frequent events (Tr = 100-200 years) and scenario H3 for very frequent events (Tr = 20-50 years). These maps are contained in the Flood Risk Management Plans (FRMP) provided by local River Basin Authorities. These multiple datasets have been merged together in a mosaic lastly updated in 2017 (Trigila et al., 2018) (most recent release at the moment of the analyses), which offers a homogeneous coverage of the entire Italian territory, although often incomplete at the basin level (minor order streams are generally neglected). Continuous updating over time is guaranteed by the Floods Directive 2007/60/EC, which requires the FRMP to be reviewed and updated every 6 years.

The example in Figure 2 shows the overlap between FRMP maps and the railway network. In particular, panel (a) depicts the Italian RSs that fall within the areas mapped by the FRMPs for the three scenarios. Panels (b) and (c) represent a zoom of the area between Turin and Vercelli (black box), displaying inundation maps (panel b) and the affected railway segments (panel c), marked with the colors corresponding to the hazard degree. RSs not directly exposed to inundations are represented in green. The proposed approach considers all the sections exposed to the different scenarios as they intersect one or more of the hazardous areas (H1, H2 and H3) identified by the District Basin Authorities.

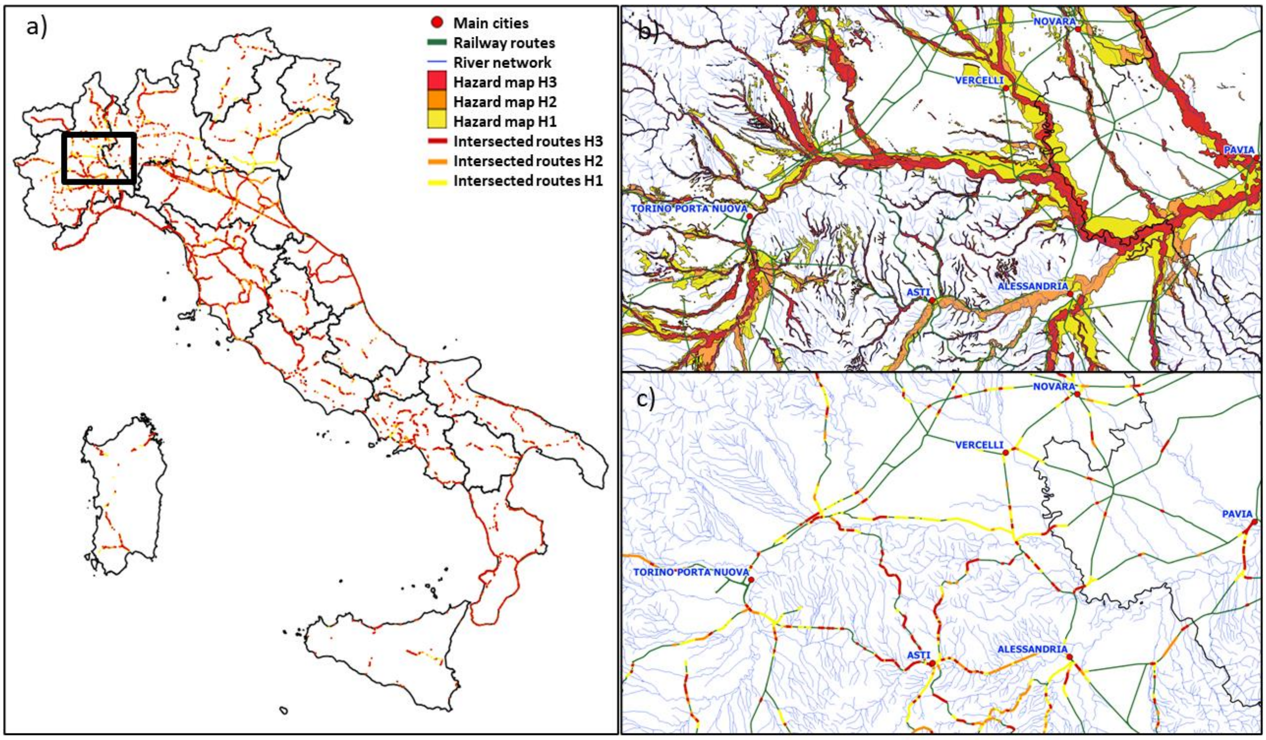

Figure 2. Panel a) Italian railway network overlapping with areas mapped by the FRMPs for various hazards levels (H1, low probability, in yellow, H2, medium probability, in orange, H3, high probability). Referring to the area within the black box, panel b) depicts the areas at risk for the FRMP; panel c) shows the segments that fall within the floodable

areas, marked with the colors corresponding to the hazard degree. The portions of railway line that do not fall into flood hazard areas are colored in green.

RSs identified as exposed to flood hazard represent the portions of network for which the assessments will be carried out. As one can notice, a single section can be exposed to multiple levels of hazard. Specifically, the sections exposed to hazard H2 are also exposed to hazard H1, i.e. they are a subset of them, while those exposed to H3 hazard are exposed to both H2 and H1 hazard. In case of exposure to multiple hazardous scenarios, the values assumed by the hydraulic parameters (e.g., water depth) are scenario-dependent. For this reason, the flood hazard assessment has to be carried out separately for the three hazard scenarios.

2.1.2 Areas not mapped in the FRMPs

In many areas, FRMPs are absent or non-exhaustive. To overcome this problem, an alternative procedure is followed to first identify the flood susceptible areas and then verify the possible presence of exposed RSs. This is achieved through a fast-processing approach based on a flood hazard indicator called Geomorphic Flood Index, GFI (Samela et al., 2017), which is derived from topographical information extracted from a DEM. It is defined as follows:

$$GFI = ln\left(\frac{h_r}{H}\right) \tag{1}$$

where h_r is a variable water level estimated for each basin location as the water depth in the closest point of the river network (along the hydrological path), while H is the difference in elevation between the location under exam and the closest point of the river network previously identified. The values of h_r are estimated as a function of the contributing area through the scaling law in Eq. (2):

$$h_r \approx bA_r^n \tag{2}$$

with A_r upslope drainage area in the river element considered, b and n scale factor and exponent (dimensionless) of the power law (see Samela et al., 2017, 2018 for further details).

Specifically, the GFI is calculated for each basin, then, the area mapped by the FRMPs (observed or simulated by hydrodynamic models) is used to calibrate a threshold binary classification, which is then applied over the unstudied areas to identify flood susceptible territories (locations with a GFI value higher than the threshold). An important advantage of the GFI method is the reduced extension of the mapped area required for its calibration. Samela et al., (2017) showed that for a reliable calibration a flood hazard map that covers at least 2% of the basin of interest is sufficient. This and other studies (Tavares da Costa et al., 2019) have shown satisfactory results in the use of this index on a large scale, despite the possible variability of the climatic, hydrological and topographical conditions of the territory. Therefore, the GFI represents a suitable method for mapping areas where detailed investigations (e.g., Hydrogeological Management Plans–PAI or FRMP) are not present (or not exhaustive), allowing the calibration of the method over neighboring and geomorphologically similar areas already mapped by the competent authorities. The GFI method is very versatile also considering DEMs of different resolution. Although the procedure benefits from high resolution (e.g., greater (lesser) DEM accuracy guarantees more (less) reliable results), Samela et al., (2018) and

Manfreda et al., (2015) have shown that DEMs normally available online, having horizontal resolution of 25-90 m, are suitable for large-scale and data scarce environments applications, suggesting the use of resolution compatible with the scale of the processes being investigated.

The FRMPs offer an almost national coverage of the main watercourses, thus those maps can be the base for the calibration of the GFI procedure. The flood susceptibility maps resulting from the application of the GFI will have hazard characteristics in accordance with the maps adopted for calibration, namely they represent a susceptibility with the same recurrence interval of the hazard map used for calibration. Since FRMPs provide maps for 3 hazard scenarios (H1, H2 and H3), the GFI maps will be characterized by the same flood frequencies.

It is worth noting that this kind of fast-processing analysis, based on geomorphological indices, does not consider the physical processes of surface water runoff (i.e., its propagation in space and time, as well as the interaction with infrastructures). However, the resulting mapping still allows a preliminary identification of critical intersections, which can then be analyzed in detail.

Once the GFI-based mapping is obtained, the sections exposed to the hazards H1, H2 and H3 are extracted in the same way described in Section 2.1.1.

2.2 Topographical and hydrological characterization of affected RSs

Railway infrastructure is evaluated by referring to a series of railway sections (RSs): any time a variation occurs on one of the main geometrical or functional characteristics of the infrastructures (e.g., n° and type of tracks, intersections, deviations, etc.) a new RS is depicted. For the scope of this work, a RS has a maximum length of 5 km.

For each RS falling within flood hazard areas, the spatial element of reference for the subsequent geomorphological and hydrological characterization are hereafter called "reference points" (red points in Figure 3). In those cases where the RS intersects the river network, reference points are identified at the intersections (Figure 3, panel a). Alternatively, in case the railway network intersects the flood hazard areas but not the river network, we adopted as reference point the closest river point along the steepest descend path from the downstream end of the infrastructure segment (see Figure 3, panel b).

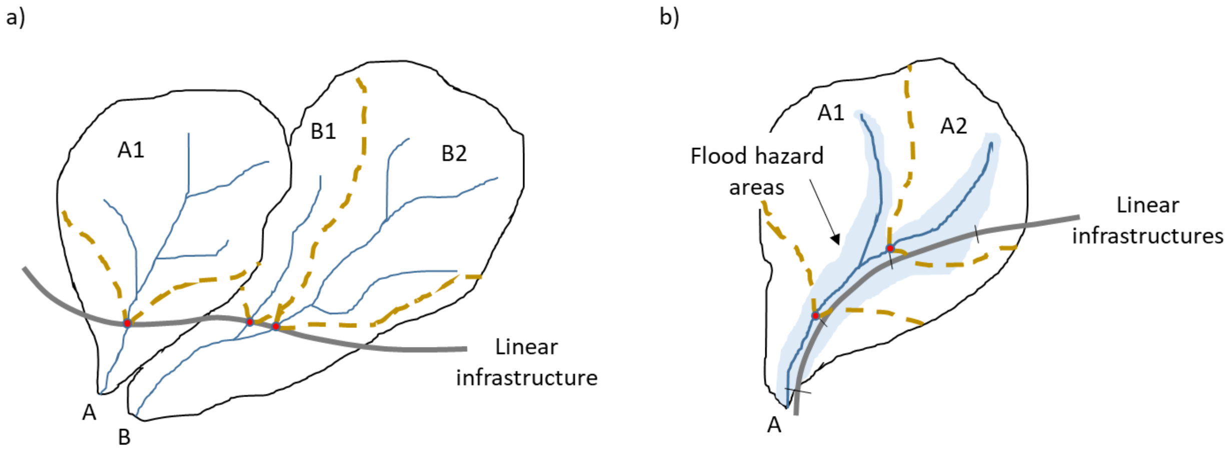

Figure 3. Scheme of the possible intersections of the railway network (grey line) with: a) the river network (blue lines); or b) the flood hazard areas (blue areas). Brown dashed lines depict the hydrographic basins closed at the reference points (red points).

2.2.1 River slope estimation

The type of flood phenomena affecting a given railway depends on the local channel slope: fast flood phenomena are typical of hilly/mountainous area, slow flood phenomena characterize valley bottom. Thus, river slope is estimated locally from the DEM considering the point of the river network closest to the RS under exam (Figure 3) and is defined as the steepest downward gradient between the cell and its 8-connected neighbors.

2.2.2 Time of concentration of the draining basins

Time of concentration (T_c) has been defined by the International Glossary of Hydrology (WMO, 1974; Beven, 2020) as the period of time required for storm runoff to flow from the most remote part of a drainage basin to the outlet. This parameter is often used to quantify the speed of formation of flood events and gives an idea of the warning time that may be available in case of intense rainfall events. This latter aspect is relevant for the railway company while evaluating the feasibility of protection/mitigation measures (such as, for example, interruption of the line, slowing down of the traffic, etc.).

T_c [hours] is evaluated for all the upslope drainage basins that contribute to the above-mentioned reference points according to Giandotti's formula (Eq. (3); Giandotti, 1934; frequently used in Italy, while alternative formulations may be adopted elsewhere):

$$T_c = \frac{4\sqrt{A}+1.5L}{0.8\sqrt{H}} \tag{3}$$

where A is the upslope contributing area of the point of interest (the reference point) [km^2], L the length of the main channel within the identified basin [km], and H the difference between the mean basin elevation and the outlet elevation [m].

The proposed methodology allows the estimation of the required variables using exclusively the DEM. Further details on T_c calculation are reported in Section 4.

2.2.3 Potential debris flows sources

The hazardous scenario associated with the possible impact against alluvial materials is predominantly related to the presence of potential source areas of debris flows near the railway, which could impact and invade the railway infrastructure. Debris flows typically occur as a result of the combination of intense rainfall, even of short duration, usually characterized by very short notice periods, over areas characterized by critical slope gradient and in presence of sediment (e.g., Pastorello et al., 2017; Horton et al., 2013). Considering the typical rapidity of these phenomena, mapping areas potentially susceptible to trigger debris flow has a fundamental role for identifying the RSs most at risk.

The scientific literature reports several methods aimed at identifying the source areas and the evolutionary dynamics of debris flows; however, only a few appear easily adoptable on a regional (or wider) scale and, consequently, of interest for the present purposes (see for example: O'Brien et al., 1993; Crosta et al., 2003; Iovine et al., 2005; Rickenmann, 2005; Pirulli and Mangeney, 2008; Iverson et al, 1998; van Westen et al., 2006; Berti and Simoni, 2007). The most suitable approaches for the purpose are those that make use of morphological and topographical parameters of the basin of interest. These methods require input data usually obtainable from DEMs or, eventually, from a few other information layers (geological or soil type maps). Among the approaches proposed in literature in the last decades (Fannin and Wise, 2001; Cavalli and Grisotto, 2006; Miller and Burnett, 2008), Pastorello et al. (2017) investigated the identification of source areas at regional scale by identifying the two most significant quantities: the local slope and the extent of the upslope contributing area (i.e. flow accumulation, which is seen as a proxy of water load) (see also Montgomery and Dietrich, 1994). As regards the second parameter, the locations of possible initiation of a debris flow are identified as those having a contributing area higher than 10 ha (Montgomery and Foufoula-Georgiou, 1993; Santos and Duarte, 2006), while, regarding the local slope, critical conditions are expected in case of slope higher than 27% (see also Takahshi, 2007; Rickenmann and Zimmermann, 1993). The reliability of these assumptions is confirmed by the good agreement between source area maps and observations collected in some basins of Northern Italy (Pastorello et al., 2017). In addition to the lower threshold value (slope>27%), an upper limit above which debris flows phenomena usually do not occur must also be defined: Cavalli et al. (2017) suggest an upper slope threshold equal to 78%, a value representative of the friction angle of the material usually affected by debris flows in the Alps. Similarly, Dai and Lee (2001) recorded a significant reduction in the occurrence of debris flows for slopes>84%, a slope threshold usually indicative of the presence of rocky material, which is not very prone to the formation of similar phenomena. Finally, Blais-Stevens and Behnia (2016) consider possible flows up to a gradient of 143%. The presence of these potential source areas in the upslope drainage area of a certain RS does not necessarily imply that the railway line will be involved in instability phenomena. In this regard, Blais-Stevens and Behnia (2016) identify the average distance traveled by a debris flow in 500 m. Starting from this consideration, and considering the inevitable uncertainty associated with these assessments, it was considered appropriate to maintain a safety margin by adopting a distance threshold value, *d* (minimum distance between the source points and the railway line), equal to at least 1 km (this value can be adjusted after inspections or more precise data depending on the area of interest). In case of sources closer to the railway line, this is considered to be exposed at risk of impact with alluvial materials. On the contrary, sources farther than 1 km are neglected.

Figure 4 shows a conceptual summary of the operational procedures adopted in this work: identification of locations with an upslope drainage area greater than 10 ha and a slope higher than 15 ° (~ 27%); as regards the last parameter, for precautionary purposes, a value of 55 ° (~ 143%; Blais-Stevens and Behnia, 2016) is adopted as the maximum slope threshold. The source points to be considered are those located within 1 km (Euclidean distance) to the railway segment. Once identified as potential source point, the hypothetical debris flows path is determined based on the maximum local slopes of the terrain. The representation scheme used is, thus, consistent with the actual evolutionary dynamics of the phenomenon.

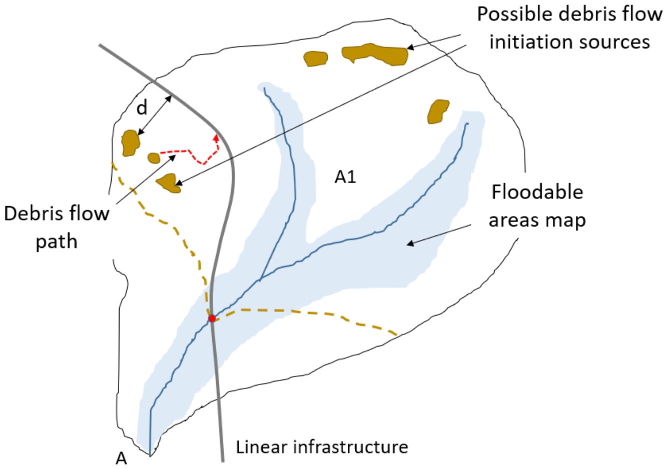

Figure 4. Railway line and possible trigger areas for debris flows.

2.3 Identification of associated damage scenarios and attribution of flood hazard classes

According to the workflow summarized in Figure 1, the last step consists in evaluating the exposure of each section to one or more damage scenarios (overtopping, infiltration, washout, impact against alluvial materials) and assigning a flood hazard class to each affected section. The values assumed by the geomorphic and hydrological parameters described in the previous subsections allow to identify the potential damage scenarios associated to each section and, consequently, to define six flood hazard classes. Criteria and thresholds for class attribution are specified in Table 1.

Table 1. Classification of flood phenomena due to the different parameters and identification of related damage scenarios.

<table>
<tr><th rowspan="2">Flood hazard class</th><th rowspan="2">Description of the flood phenomena</th><th rowspan="2">River slope</th><th rowspan="2">Sub-basin time of concentration</th><th rowspan="2">Debris flow phenomena</th><th rowspan="2">Geo-morphological parameters for debris flow initiation sources</th><th colspan="4">Damage scenarios</th></tr>
<tr><th>Overtopping (A)</th><th>Infiltration (B)</th><th>Washout (C)</th><th>Impact against alluvial materials (D)</th></tr>
<tr><td>I</td><td>Hill/mountain flood phenomena with potential debris flow sources</td><td rowspan="2">> 4%</td><td rowspan="2">A few hours</td><td>Yes</td><td>Contributing area > 10 ha and slopes angle > 27%</td><td>X</td><td></td><td></td><td>X</td></tr>
<tr><td>II</td><td>Hill/mountain flood phenomena without debris flow</td><td>No</td><td>Contributing area ≤ 10 ha and/or slopes angle ≤ 27%</td><td>X</td><td></td><td></td><td></td></tr>
<tr><td>III</td><td>Rapid flood phenomena with potential debris flow sources</td><td rowspan="2">< 4%</td><td rowspan="2">< 12 hours</td><td>Yes</td><td>Contributing area > 10 ha and slopes angle > 27%</td><td>X</td><td>X</td><td>X</td><td>X</td></tr>
<tr><td>IV</td><td>Rapid flood phenomena without debris flow</td><td>No</td><td>Contributing area ≤ 10 ha and/or slopes angle ≤ 27%</td><td>X</td><td>X</td><td>X</td><td></td></tr>
<tr><td>V</td><td>Slow flood phenomena with potential debris flow sources</td><td rowspan="2">< 4%</td><td rowspan="2">≥ 12 hours</td><td>Yes</td><td>Contributing area > 10 ha and slopes angle > 27%</td><td>X</td><td>X</td><td>X</td><td>X</td></tr>
<tr><td>VI</td><td>Slow flood phenomena without debris-flow</td><td>No</td><td>Contributing area ≤ 10 ha and/or slopes angle ≤ 27%</td><td>X</td><td>X</td><td>X</td><td></td></tr>
</table>

To further clarify the proposed classification, the tree diagram in Figure 5 illustrates the expected flooding phenomena and, thus, the consequent flood hazard class attribution, depending on whether or not predefined thresholds for the geomorphic and hydrological parameters described in the previous subsections are exceeded.

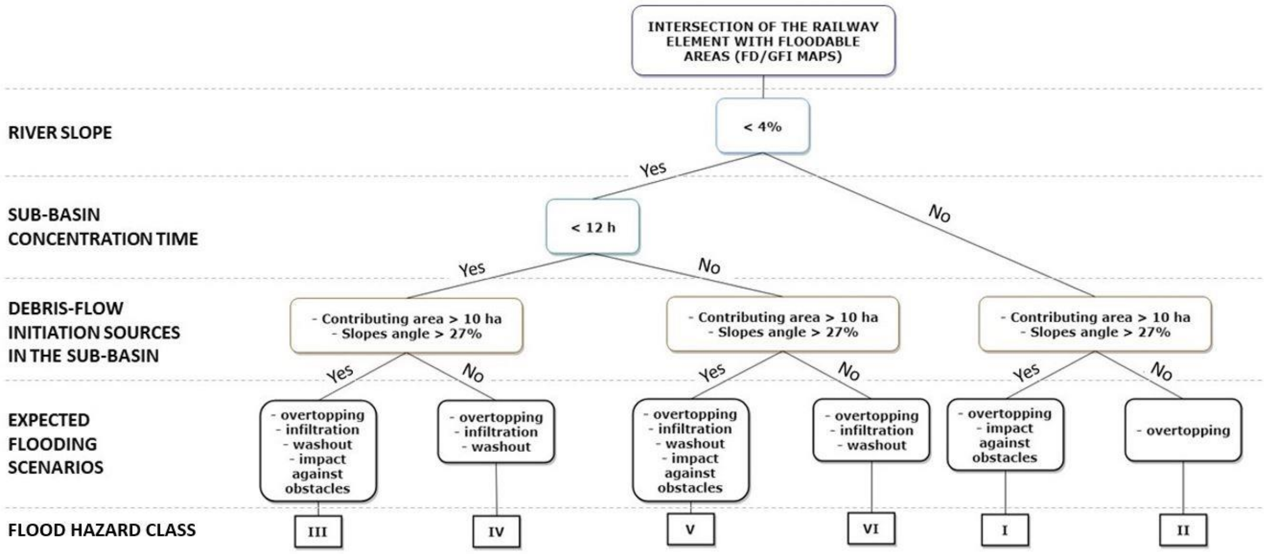

Figure 5. Tree diagram showing the classification of flood phenomena with the possible associated damage scenarios.

2.4 Potential application for detailed damage scenario description

Overtopping, infiltration, washout and impact against alluvial materials are potential damage scenarios to which RSs might be subject in the event of a flood, depending on the geomorphic and hydraulic parameters previous described. However, activation and intensity of such scenarios depends on both hydraulic load and tracks characteristics (i.e., tracks elevation relative to the ground level, trackbed shape and materials, etc.). To check for critical sections, and rank the priorities of intervention, a more detailed analysis is needed, which considers the geometrical characteristics of railways track (if possible based on a high-resolution DSM – Digital Surface Model) together with hydraulic and geotechnical parameters driving the critical phenomena (e.g. water depth for overtopping, hydraulic gradient for piping, etc.).

Among the most critical scenarios for railways transport there is the track impairment caused by trackbed overtopping, which is chosen as an example to show the potential use of the methodological framework presented in this work. Similar considerations can be done also for other damage scenarios (e.g., infiltration, washout, etc.), in relation to their specific hydraulic descriptors. According to the guidelines currently in use by RFI, the railway is considered critical as regards overtopping if Eq. 4 is satisfied:

$$\Delta h = h_{pf} - h_w < 2.5m \qquad (4)$$

where Δh represents the freeboard, h_{pf} is the height of the rail and h_w the water depth. A quite cautionary 2.5 m threshold is chosen to consider the significant uncertainty associated to the estimates of the water depth.

For each RS falling in areas mapped by the FRMPs, or using the GFI approach, the methodology requires the identification of the water depth associated to the reference point for the different hazard scenarios (H1, H2 and H3). According to the presented methodology, the water depth for different hazards is estimated in a simplified way by exploiting the elevations of the DEM at the edge of the inundated areas (Figure 6). Specifically, a DEM-section is drawn across the inundation extent in correspondence of each reference point. The elevations of the DEM at the two inundation edges are linearly interpolated (blue points) along the drawn line: the water depth is estimated at the reference point, that corresponds to the railway location (yellow point in Figure 6), in relation to the ground elevation (see Figure 6).

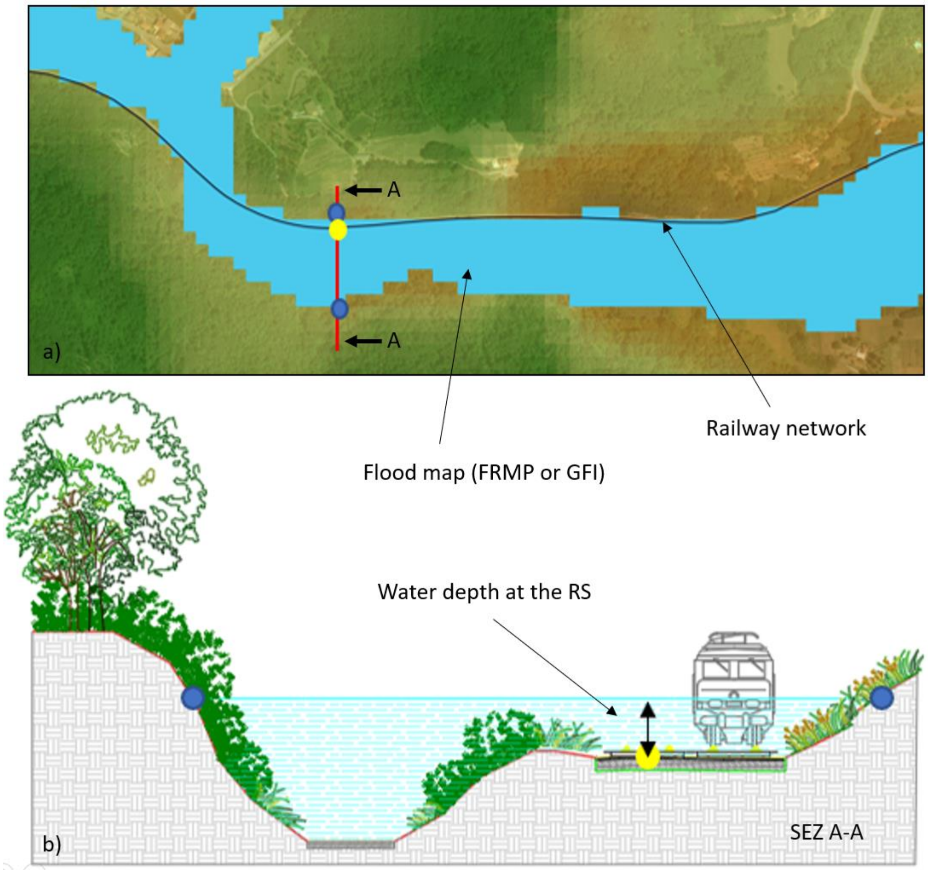

Figure 6. Conceptual scheme for the simplified determination of the water depths over inundated RS: plan representation in panel a) and section representation in panel b). The yellow point in both panels indicates the reference point of the analyzed RS. The red line represents the terrain profile through the reference point. Blue points indicate the inundation edges obtained intersecting the inundation extent with the DEM.

It is worth mentioning that it is not necessary to resort to this simplified approach when expected water depths are provided by competent Authorities. Once the water depth is identified, it can be compared with the height of the rail and the verification of the freeboard is soon completed. Similarly, water depth estimates might be used for evaluating the potential activation of other hydraulic damage scenarios (e.g., piping activation across the trackbed), in accordance to expert-based guidelines in use by RFI.

3. Case studies and dataset

The described methodology has been tested on several basins in Italy (Figure 7). Case studies have been selected across the country, including both flat and hilly areas. Five river basins (Dora Baltea, Tronto, Aulella, Paglia and Basento) have been investigated considering RS s falling into flood hazard areas as identified by the FRMPs (three scenarios H1, H2 and H3) (Figure 7, panel a)). Five river basins (Chienti, Torto, Aulella, Paglia and Basento) partially covered by FRMP mapping have been analyzed using the GFI technique (Figure

7, panel b)). Among them, three basins (Aulella, Paglia and Basento) have been studied with both inundation delineations (FRMP and GFI) for comparison purposes and to emphasize the potential improvements obtainable by applying the GFI method.

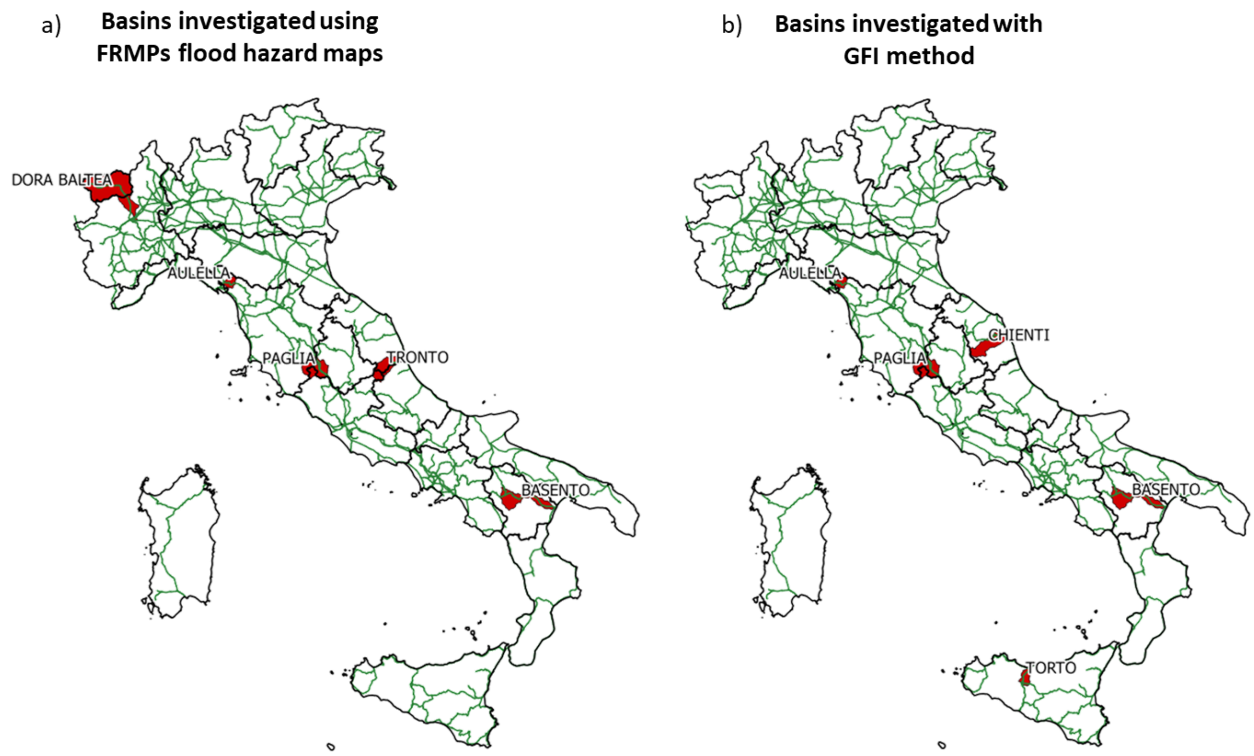

Figure 7. Geographical setting of the case studies: panel a) depicts the selected basins containing railway intersecting flood hazard areas mapped in the FRMP; panel b) shows the selected basins with sections falling in areas not mapped in the FRMP and studied with the GFI approach. The study basins are colored in red, the railway network in green.

Several data and information layers have been exploited for the analysis of flood hazard along railway infrastructures, which are summarized below:

- national coverage of railways and stations, containing information relating to the position and characteristics of each element, such as the type (number of tracks; type of embankment, etc.) (vector files provided by RFI).

- Digital Elevation Model (DEM) with national coverage at 20 m resolution (from SINAnet, ISPRA; see Data availability section).

- National coverage of main and secondary hydrographic basins, and hydrographic network, obtained from the SINAnet of the ISPRA.

- National coverage of the FRMP flood hazard maps derived for three return periods (Tr): H1 (Tr up to 500 years), H2 (Tr = 100-200 years) and H3 (Tr = 20-50 years); maps updated to 2017 SINAnet website.

4. Results and discussion

4.1 Flood hazard class attribution

This Section illustrates in detail the results obtained for the Paglia basin (1404 km^2, including approximately 110 km of infrastructure), which was one of the case studies analyzed using both FRMP and GFI maps. It also provides an overview of the most significant findings obtained over the other selected basins.

Figure 8, panel a) represents the hydrologically conditioned DEM; panel b) the derived flow directions; panel c) the flow accumulation. Panels d), e), f) show respectively in yellow, orange and red the RSs falling in flood-prone areas for hazard scenarios H1, H2 and H3 according to the FRMP maps; the remaining part of the railways network is shown in grey. Cyan points in panel d, e, f) represent the reference points of each section.

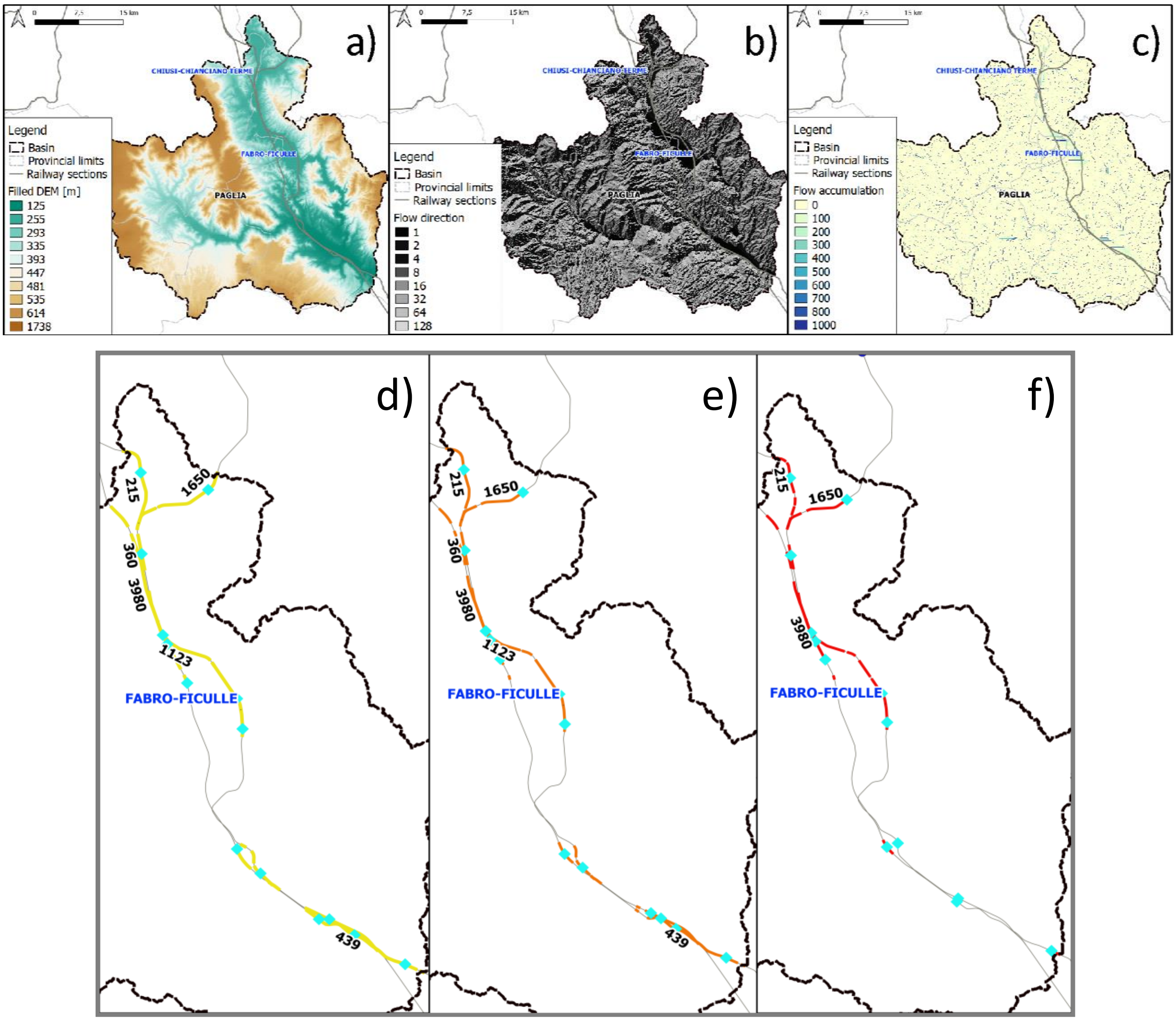

Figure 8. Paglia case study. Panel a): Conditioned DEM; b): flow direction; c): flow accumulation; d), e), f): RSs falling in areas mapped by the FRMP with associated hazard H1 (yellow), H2 (orange) and H3 (red), respectively. The cyan dots represent the reference points and the outlets of the upslope drainage basins of each section.

Starting from the information described, river slope, time of concentration and potential debris flows occurrence were evaluated at each reference point. Also, water depths at the same locations were estimated (according to Section 2.4). Although evaluated for all flood scenarios, for the sake of brevity, Table 2 only reports the results for the intermediate hazard scenario H2, which designation is important because it describes frequent events and is often adopted as the standard for flood protection measure design and floodplain management regulations.

Table 2. Classification of RSs exposed to the flood hazard scenario H2 according to the FRMP and GFI in the Paglia river basin. In italic the variables used for defining the flood hazard class. RSs identified as exposed by the GFI analysis only are highlighted with a grey background.

	FRMP - H2						***GFI - H2***					
ID	***River slope [%]***	**Sub-basin surface [km^2]**	***T_c [h]***	***Debris-flow [Y/N]***	**Water depth [m]**	**Flood hazard class**	***River slope [%]***	**Sub-basin surface [km^2]**	***T_c [h]***	***Debris-flow [Y/N]***	**Water depth [m]**	**Flood hazard class**
215	<1‰	2.61	1.61	NO	8.40	IV	<1‰	2.61	1.61	NO	5.75	IV
241	<1‰	3.86	0.99	NO	< 0.05	IV	<1‰	674.77	12.30	YES	11.60	V
360	<1‰	95.84	9.28	YES	2.50	III	<1‰	95.84	9.28	YES	2.09	III
439	0.04	48.65	3.08	YES	< 0.05	III	0.05	48.65	3.08	YES	6.26	I
668	-	-	-	-	-	-	<1‰	696.74	12.63	YES	5.83	V
1123	<1‰	289.71	12.64	YES	< 0.05	V	<1‰	289.57	12.62	YES	10.67	V
1614	0.05	22.46	2.55	YES	< 0.05	I	0.15	22.46	2.56	YES	23.12	I
1650	0.07	11.11	3.23	YES	4.29	I	<1‰	34.36	7.89	YES	10.34	III
1882	0.25	1.12	0.87	YES	< 0.05	I	0.05	48.64	2.99	YES	25.72	I
2027	<1‰	233.78	11.88	NO	< 0.05	IV	0.10	30.92	3.37	YES	9.86	I
2055	<1‰	5.30	1.92	YES	< 0.05	III	<1‰	20.32	3.52	YES	0.60	III
2466	0.04	1.64	0.73	YES	6.26	III	<1‰	634.52	11.91	YES	3.32	III
2450	-	-	-	-	-	-	<1‰	1365.01	17.47	YES	17.35	V
2752	0.07	11.95	2.20	YES	0.00	I	0.05	11.95	2.20	YES	15.00	I
3142	<1‰	4.25	2.44	NO	< 0.05	IV	<1‰	211.98	11.02	YES	8.48	III
3285	-	-	-	-	-	-	<1‰	11.42	2.13	YES	3.67	III
3980	<1‰	212.08	10.84	YES	< 0.05	III	<1‰	212.08	10.84	YES	14.95	III

Table 3 reports the metrics obtained in calibrating the linear binary classification based on the GFI for the Paglia river basin for the H2 scenario. The calibration is carried out comparing, cell by cell, the GFI flood-prone/flood-free areas with the FRMP flood hazard maps, obtaining a contingency table and performance metrics.

Table 3. Performance measures obtained in calibrating the linear binary classification based on the GFI for the Paglia river basin. The Area Under the Receiver Operating Characteristics curve (AUROC) value that aggregates the performance of the classifier at all threshold values is also reported.

Paglia River Basin – H2				
True Positive Rate RTP	False Negative Rate RFN	True Negative Rate RTN	False Positive Rate RFP	Area Under the ROC curve AUROC
90%	10%	75%	25%	0.87

Figure 9a shows the spatial distribution of the GFI in the Paglia basin; Figure 9b illustrates the flood hazard map according to the FRMP (specifically, H2 is shown) that was used to calibrate the GFI binary classification and identify the flood-prone areas for each hazard scenario; Figure 9c represents the GFI flood-prone areas for the H2 hazard scenario.

Predicted flood-prone areas have a very high True Positive Rate (RTP) (90% of the raster cells are correctly identified as flood-prone). On the other hand, the False Positive Rate (FPR) of 25% obtained for the Paglia basin shows a tendency to over predict flood-prone areas.

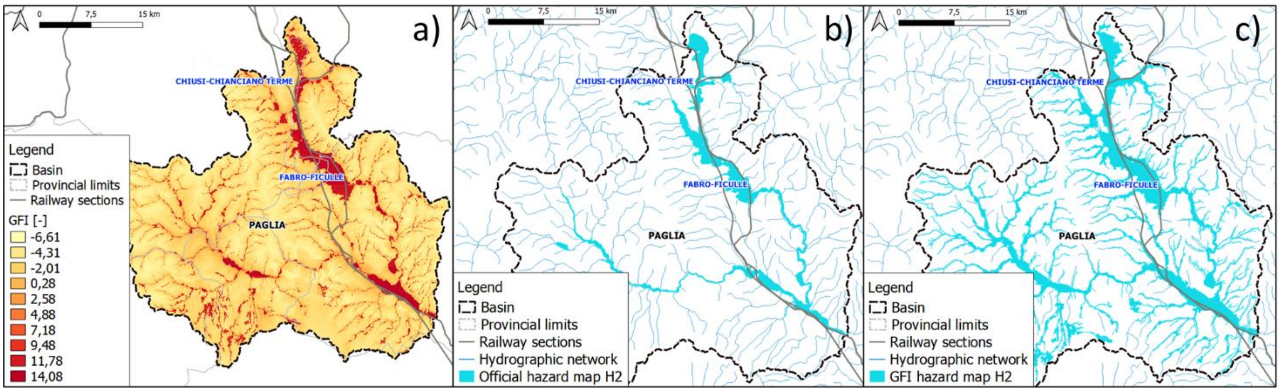

Figure 9. Panel a): spatial distribution of the GFI in the Paglia river basin; b): FRMP mapping of H2 hazard scenario, used for the calibration of the GFI method; c): resulting flood-prone areas map for the H2 hazard scenario according to the GFI approach.

Table 2 also reports the results of the analysis performed on the Paglia river basin with the GFI approach.

Looking at results, it can be noticed how the greater extent of the river network investigated with the GFI approach translates into an increase in the number of exposed RSs. In addition, the flood hazard class attributed to a given section may vary in relation to the adopted approach. As a matter of fact, a different inundation extent may result in the identification of different reference points, thus potentially different slopes (e.g. RSs 439, 1650), drained basins and exposure to debris flow phenomena (e.g., RSs 241, 2027). This also entails differences in terms of Tc and water depth. In particular, changes in the flood extent delineation and consequent intersection with different portions of RSs result in different hydrological parameter estimations (see also eq. 3) and thus in different Tc values (e.g., longer Tc adopting the GFI in one-third of the cases along the Paglia basin).

Concerning the water depth, in general, GFI tends to overestimate compared to FRMP, where inundation map is typically derived from more detailed investigations (i.e., hydraulic modeling; see e.g. Manfreda and Samela, 2019). Although a direct comparison of RSs having the same ID could be misleading for the reasons mentioned above, water depth values for GFI appear significantly higher than those retrieved from FRMP. Among the different reasons, this appears to be mainly due to the simplified approach adopted in this case. Conceptual scheme in Figure 6 provides an intuitive explanation, highlighting how the topography of the valley surrounding the river network may be responsible for such differences. This aspect represents a limitation of the current approach to be aware of in case the values of the expected water depth might be used for more detailed investigations. Future methodological development will deal with this particular issue.

For each hazard scenario, Figure 10 graphically shows the comparison between the flood risk classes obtained in the Paglia basin using the FRMP maps (panels a, b, c) and those obtained using the GFI maps (panels d, e, f). Sections are mapped with different colors according to the different classes.

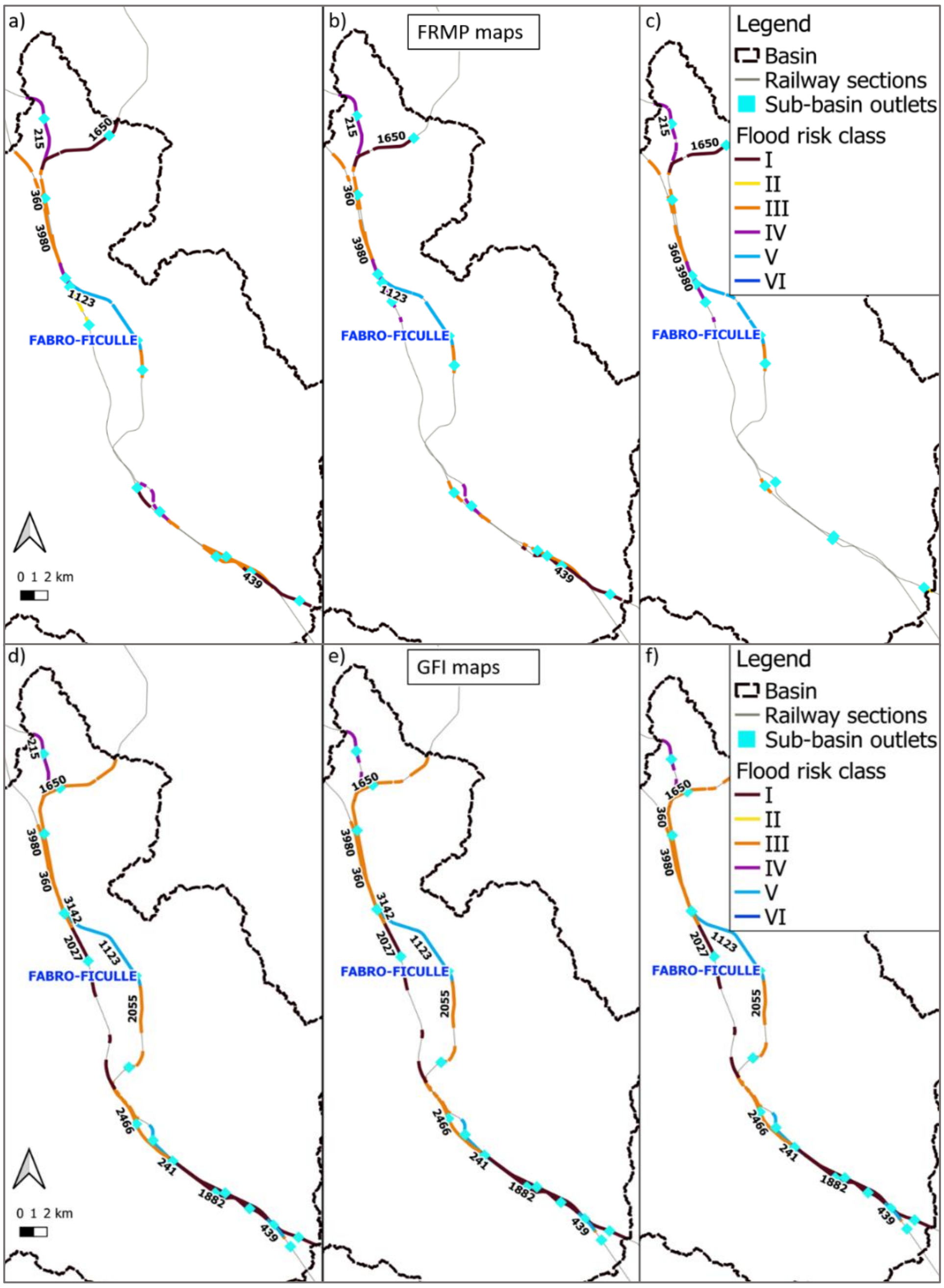

Figure 10. Classification of the sections based on the expected alluvial phenomena in the Paglia basin, according to the FRMPs for the hazard scenarios H1, H2 and H3 (respectively: panels a, b, c), and according to the GFI procedure for the hazard scenarios H1, H2 and H3 (respectively: panels d, e, f). Not classified sections are depicted in green.

From Figure 10 it is worth noting that the railway line exposed to flood hazard according to GFI mapping is more extended than the one obtained using the FRMP maps. The same consideration emerged in all the five basins investigated with the GFI method. Although they are not described in detail for the sake of brevity, the most meaningful findings are summarized in the following Table 4 and Table 5. Specifically, Table 4 shows how the flood hazard areas identified by the GFI procedure are significantly larger than the ones spotted in the official maps. This can be attributed to different reasons: i) in general, GFI seems to overestimate the flood inundation extent (this is in line with previous findings; e.g., Manfreda and Samela., 2019; Samela et al., 2017); ii) the inclusion of the minor order river network ensured by this method, which are often neglected in FRMP maps. Accordingly, the exposed railway line in terms of linear extent, reported in Table 5, results much higher for the GFI analysis for all the case studies.

Table 4. Areas [km^2] identified as potentially affected by floods according to FRMP and GFI maps for all the case studies.

Case study	River basin	Basin surface [km^2]	Floodable surface - H1 [km^2]		Floodable surface - H2 [km^2]		Floodable surface - H3 [km^2]	
			FRMP	GFI	FRMP	GFI	FRMP	GFI
1	Aulella	408.3	7.91	38.48	6.95	38.13	5.54	35.22
2	Paglia	1403.8	87.75	224.89	70.33	200.34	55.29	200.34
4	Basento	1552.8	63.55	166.71	59.77	166.71	48.01	157.12

Table 5. Linear extent (in km) of RSs potentially affected by floods according to FRMPs and GFI maps for all the case studies.

Case study	River basin	Basin surface [km^2]	Affected infrastructures H1 [km]		Affected infrastructures H2 [km]		Affected infrastructures H3 [km]	
			FRMP	GFI	FRMP	GFI	FRMP	GFI
1	Aulella	408.3	8.74	21.75	6.98	21.49	6.24	21.07
2	Paglia	1403.8	64.27	87.71	54.93	82.73	35.34	82.73
4	Basento	1552.8	36.22	82.29	28.21	82.29	19.41	77.19

A comprehensive summary of the analysis performed over all the investigated basins (5 with the FRMPs maps and 5 using the GFI method) is reported in Table 6, which provides the total number of affected RSs in each basin, and how they rank in each flood hazard class. The three basins investigated using both methods (indicated with grey background) corroborate what observed in the Paglia basin: exploring larger areas and longer railway segments brings to the identification of an increased number of potentially affected RSs.

Table 6. Number of RSs for each flood hazard class (and their percentage with respect to the total exposed infrastructure) for the five case studies investigated on the basis of the FRMP (hazard scenario H2) and for the five case studies investigated with the GFI approach. The three basins in common are highlighted with a grey background. The last column reports the total number of exposed sections.

FRMP- H2

Case study	River basin	No. of sections in class I (% of total)	No. of sections in class II (% of total)	No. of sections in class III (% of total)	No. of sections in class IV (% of total)	No. of sections in class V (% of total)	No. of sections in class VI (% of total)	Total exposed sections
1	Aulella	3 50%	0 0%	2 33.3%	1 16.7%	0 0%	0 0%	6
2	Paglia	4 28.6%	0 0%	5 35.7%	4 28.6%	1 7.1%	0 0%	14
3	Basento	4 30.8%	0 0%	5 38.5%	1 7.7%	2 15.4%	1 7.7%	13
4	Dora Baltea	13 48.1%	2 7.4%	5 18.5%	1 3.7%	5 18.5%	1 3.7%	27
5	Tronto	3 33.3%	0 0%	1 11.1%	3 33.3%	0 0%	2 22.2%	9
Total		27 39.1%	2 2.9%	18 26.1%	10 14.5%	8 11.6%	4 5.8%	69

GFI - H2

Case study	River basin	No. of sections in class I (% of total)	No. of sections in class II (% of total)	No. of sections in class III (% of total)	No. of sections in class IV (% of total)	No. of sections in class V (% of total)	No. of sections in class VI (% of total)	Total exposed sections
1	Aulella	5 50%	1 10%	4 40%	0 0%	0 0%	0 0%	10
2	Paglia	5 29.4%	0 0%	7 41.2%	1 5.9%	4 23.5%	0 0%	17
3	Basento	6 33.3%	0 0%	10 55.6%	0 0%	2 11.1%	0 0%	18
4	Torto	5 50%	0 0%	3 30%	2 20%	0 0%	0 0%	10
5	Chienti	3 37.5%	3 37.5%	0 0%	2 25.0%	0 0%	0 0%	8
Total		24 38.1%	4 6.3%	24 38.1%	5 7.9%	6 9.5%	0 0%	63

4.2 Validation against historical flood events and procedure limitations

With the intent of providing evidence on the value of the proposed methodology, we validated our results by comparing the RSs resulting exposed to flood hazard to historical records of critical conditions attributable to fluvial or pluvial flood scenarios. Memories of past critical conditions were collected with the support of RFI referring to the 2001-2014 period for the three basins where both FRMP and GFI maps were used. The H2 hazard scenario has been chosen again being the one of major operational interest. In the three basins investigated with both methodologies, we looked for recorded flood events and then we verified how many of them involved RSs labelled as exposed according to our analyses. The recorded events are shown with blue dots in Figure 11. Panels of Figure 11 show the overlap between the location of the historical flood events and the RSs belonging to the different classes or not classified for: a) Paglia, b) Basento and c) Aulella basins.

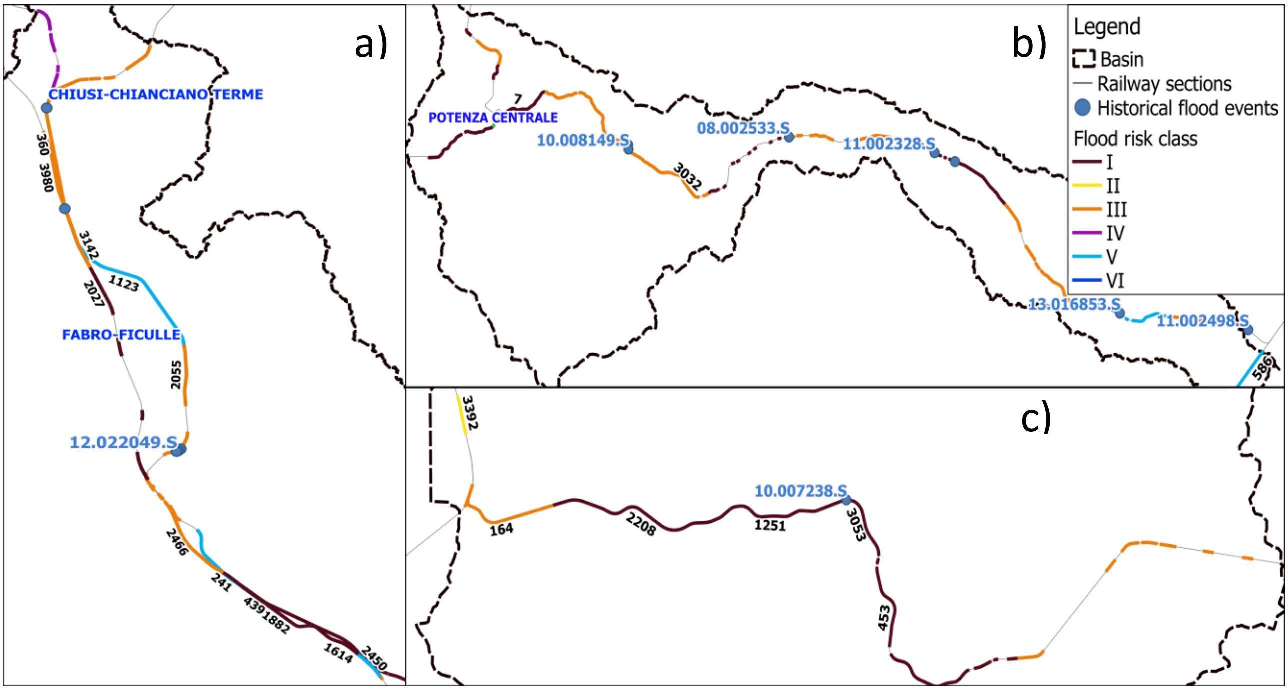

Figure 11. Comparison of exposed sections and recorded local inundations for Paglia, Basento and Aulella basins (panels a), b) and c), respectively). The spatial geolocation of the historical flood events is depicted with blue dots. RSs found to be at risk according to the analysis with the GFI approach (H2 scenario) are represented in different colors according to their flood hazard class; the non-classified portion of the railway network is represented by the grey line.

Table 7 shows the results of this comparison, reporting the percentage of real events occurred along exposed sections with respect to the total. The events that occurred at railway stations were referred to the RS immediately upstream. Results highlight how the GFI approach ensures a wider identification of sections potentially affected by hydrological events. As a matter of fact, some of the locations affected by these phenomena in the past have been properly spotted with the GFI approach, while neglected by the analysis performed adopting FRMP maps. It is also possible to note the failure of both methods in identifying additional places affected by flood events. This might be due to the fact that among the hydrological events recorded as "alluvial", together with riverine floods, also pluvial inundation caused by local convective meteoric phenomena are included. Evidently, those latter events cannot be described by the methodology reported here.

In addition, it is worth mentioning that a fast-processing geomorphologic approach, as the one tested, is certainly approximated with respect of performing hydrologic-hydraulic modelling. Nevertheless, the information obtained can be useful to target the investments on the critical points of the railway line and appropriately prioritize additional detailed analyses and interventions.

Furthermore, the level of accuracy ensured by the approach is expected to increase adopting input data of higher precision: the availability of high resolution DEM, or DSM (Digital Surface Model), would allow to considerably reduce the uncertainty in the results and obtain a more realistic information on the state of the railway line, allowing to provide assessments not only on the hazard of each section, but also on its actual exposure to the different damage scenarios (overtopping, infiltration, washout, impact against alluvial materials).

Concerning debris flow, the identification of the triggering areas and flow paths is carried out by exploiting exclusively topographic information, which can be derived from the DEM (i.e., flow accumulation and slope). Though suitable for large scale investigation and validated in previous studies (see e.g., Pastorello et al., 2017), it is worth noting that the adopted approach presents elements of uncertainty and margins of improvement. Potential threshold distinction in relation to other distinctive parameters (e.g., topographic, geologic, soil or land cover type, etc.) is not provided in the literature (to the best of our knowledge), yet. Nevertheless, such possibility might enhance the approach accuracy, especially for the definition of debris flow dynamics, which is likely to appear more sensitive to those parameters compared to the identification of triggering areas. That said, the range of the adopted threshold is considered to be wide enough to appear prudential in the identification of the triggering areas, which sounds appropriate for the scope of the overall investigation framework. Additional and more detailed analysis will be eventually planned for the basins where debris flow risk appears more severe.

Table 7. Historical flood events recorded in the years 2001-2014 that affected the railway network in the 3 basins investigated on the basis of both official FRMP maps and GFI method; the total number of events and the number of events occurring on exposed sections are reported (hazard scenario H2).

FRMP – H2				
River basin	**No. of recorded historical flood events**	**No. of exposed sections**	**% of events on exposed sections**	**Hazard class of the involved sections**
Aulella	1	1	100%	I
Paglia	5	2	40%	III
Basento	12	3	25%	III, I
GFI – H2				
River basin	**No. of recorded historical flood events**	**No. of exposed sections**	**% of events on exposed sections**	**Hazard class of the involved sections**
Aulella	1	1	100%	I
Paglia	5	3	60%	III
Basento	12	6	50%	I, III

5. Conclusions

The present paper illustrates a fast-processing methodology for large-scale assessment of flood hazard on transport infrastructure, with a focus on rail networks. The developed methodology is based on the use of geomorphological variables, which can be inferred through specific analyses from a DEM of adequate spatial resolution. Specifically, the methodology carried out enables:

- The identification of the network segments (railway sections, RSs) that are prone to different flood hazard scenarios (H1, low probability; H2, medium probability; H3, high probability) by using the official

FRMP maps. The obtained result is a homogeneous mapping, with a potential national coverage, based on the most recent information (FRMP 2017).

- The development of an investigation algorithm to identify potentially floodable areas, for various return periods, that represents a completion and an alternative to the use of the official maps offered by the River Basin Authorities. This approach is based on the Geomorphic Flood Index (GFI), which considers exclusively the topographic characteristics of the area of interest and is able to offer a more extensive mapping of the flood susceptible areas, also considering the minor order river network, largely neglected in the existing flood hazard maps (PAI, FRMP). This alternative mapping enables the identification of flood-related hazards for RSss located in areas not yet investigated by the FRMP.

- Advancements on the evaluation of the hydrological characteristic of the expected flood events through the estimation of the time of concentration of the drainage basins closed at the RSs of interest.

- Extension towards the identification of RSs that can be potentially affected by the impact with alluvial materials (debris-flow), which triggering locations and paths are estimated based on the topographical characteristics of the area of interest.

- The development of an algorithm for a preliminary evaluation of the water depth expected at the flooded RSs, useful to evaluate the risk of overtopping of the railway network in case of the availability of more detailed information about the rail height or a high-resolution DSM.

The proposed methodology was applied and tested over seven Italian basins, only partially considered in the FRMPs, and considering three hazard scenarios (H1, H2 and H3). To perform a first validation of the procedure reliability, the results were compared with historical flood events that involved the railway infrastructure. Results were found to be in line with the experiences and observations reported by RFI (network manager) regarding the occurrence of slowdowns or service interruptions, defining the result of the application satisfactory. The methodology is suitable for assessing the criticality of sections and estimating a ranking of intervention priorities, which could be useful for planning hazard mitigation interventions and measures to be adopted during the event. Additional investigations will be carried out in the next future to test the performances of the proposed methodological framework in different hydrological/morphological conditions.

This simplified methodology represents a useful tool for the assessment of the classes of inundation and mass-movement phenomena for sections that intersect areas at risk of flooding, whether they are already mapped or not in official basin planning tools. The study showed how the GFI procedure can be adopted to extend the mapping where official maps are non-exhaustive or completely lacking. The strength of the methodology resides on its applicability to any hazard scenario and study area, requiring only a DEM of adequate resolution (i.e., 20 m in our study) and some reliable information for small portions of the area of interest (for calibration purpose).

Concluding, the presented study has led to the identification of useful tools and methodologies for a rapid and homogeneous identification, potentially suitable for large spatial scales application, of RSs prone to water-related hazards, which represents a first step of the process intended to assess and mitigate the overall flood-related risk for the railway network. Future investigations will combine current hazard assessment with network exposure (n° of trains, passengers, cargo, etc.) and vulnerability assessment leading to the identification of risk reduction measures.

Furthermore, the methodology is flexible and, with appropriate adaptations, suitable to perform analyses of other transport networks (e.g., road infrastructures).

Data availability

DEM, hydrographic basins and hydrographic network, as well as FRMP flood hazard maps are available from the National Environmental Information System Network (SINAnet) of the Italian Institute for Environmental Protection and Research (ISPRA) (http://www.sinanet.isprambiente.it/it/sia-ispra/download-mais/dem20/view) upon registration.

Acknowledgments

Authors are extremely grateful to Dr. Francesco Dottori, one additional anonymous Reviewer and the Associate Editor for their meaningful comments.

Funding details

This work was supported by Rete Ferroviaria Italiana S.p.A., (research contract n. 142/2018).

References

Berti, M., & Simoni, A. (2007). Prediction of debris flow inundation areas using empirical mobility relationships. Geomorphology, 90(1-2), 144-161.

Beven, K. J. (2020). A history of the concept of time of concentration. Hydrology and Earth System Sciences, 24(5), 2655-2670.

Blais-Stevens, A., Behnia, P. (2016). Debris flow susceptibility mapping using a qualitative heuristic method and Flow-R along the Yukon Alaska Highway Corridor, Canada. Natural Hazards and Earth System Sciences, 16(2), 449-462.

Blöschl, G., Hall, J., Viglione, A., Perdigão, R. A., Parajka, J., Merz, B., ... & Boháč, M. (2019). Changing climate both increases and decreases European river floods. Nature, 573(7772), 108-111.Bouwer, L.M., Bubeck, P., Aerts, J.C.J.H., 2010. Changes in future flood risk due to climate and development in a Dutch polder area. Glob. Environ. Change 20 (3), 463–471.

Cavalli, M., Crema, S., Trevisani, S., Marchi, L. (2017). GIS tools for preliminary debris-flow assessment at regional scale. Journal of Mountain Science, 14(12), 2498-2510.

Cavalli, M., Grisotto, S. (2006). Individuazione con metodi GIS delle aste torrentizie soggette a colate detritiche: applicazione al bacino dell'alto Avisio (Trento). Nuova Bios, Idronomia Montana, 26, 1-11.

Chang, H., Lafrenz, M., Jung, I. W., Figliozzi, M., Platman, D., & Pederson, C. (2010). Potential impacts of climate change on flood-induced travel disruptions: a case study of Portland, Oregon, USA. Annals of the Association of American Geographers, 100(4), 938-952.

CRED, UNDRR (2020). Human Cost of Disasters. An Overview of the last 20 years: 2000–2019. https://reliefweb.int/report/world/human-cost-disasters-overview-last-20-years-2000-2019 (UNDRR, 2020).

Crosta, G. B., Imposimato, S., Roddeman, D. G. (2003). Numerical modelling of large landslides stability and runout. Natural Hazards and Earth System Science, 3(6), 523-538.

Dai, F. C., Lee, C. F. (2001). Terrain-based mapping of landslide susceptibility using a geographical information system: a case study. Canadian Geotechnical Journal, 38(5), 911-923.

Dawson, R.J., Gosling, S., Chapman, L., Darch, G., Watson, G., Powrie, W., Bell, S., Paulson, K., Hughes, P., Wood, R., Thompson, D., Johns, D., (2016). Chapter 4: Infrastructure in UK Climate Change Risk Assessment 2017 (CCRA 2017). In: Adaptation Sub-Committee (ASC) of the Committee on Climate Change, London (UK).

De Moel, H., Aerts, J. C., & Koomen, E. (2011). Development of flood exposure in the Netherlands during the 20th and 21st century. Global Environmental Change, 21(2), 620-627.

Domeneghetti, A., Carisi, F., Castellarin, A., & Brath, A. (2015). Evolution of flood risk over large areas: Quantitative assessment for the Po river. Journal of Hydrology, 527, 809-823.

Dunn, S., Fu, G., Wilkinson, S., Dawson, R. (2013). Network Theory for Infrastructure Systems Modelling, Proceedings of the institution of Civil Engineer - Engineering Sustainability, 166(5), 281-292.

Fannin, R. J., Wise, M. P. (2001). An empirical-statistical model for debris flow travel distance. Canadian Geotechnical Journal, 38(5), 982-994.

Firmi, P., Iacobini, F., Rinaldi, A., Vecchi, A., Agostino, I., & Mauro, A. (2021). Methods for managing hydrogeological and seismic hazards on the Italian railway infrastructure. Structure and Infrastructure Engineering, 17(12), 1651-1666.

Giandotti, M. (1934). Previsione delle piene e delle magre dei corsi d'acqua, Memorie e studi idrografici, Pubbl. 2 del Servizio Idrografico Italiano: Rome, Italy, Vol. VIII, 107.

Gil, J., & Steinbach, P. (2008). From flood risk to indirect flood impact: evaluation of street network performance for effective management, response and repair. WIT Transactions on Ecology and the Environment, 118, 335-344.

Guikema, S.D. (2009). Natural disaster risk analysis for critical infrastructure systems: An approach based on statistical learning theory, Reliability Engineering & System Safety, 94(4), 855-860.

Guze, S. (2014). Graph theory approach to transportation system design and optimization, TransNav, 8 (4), 571-598.

Hall, J.W., Sayers, P.B., Dawson, R.J. (2005). National-scale assessment of current and future flood risk in England and Wales. Nat. Hazards 36, 147–164.

Hong, L., Ouyang, M., Peeta, S., He, X., & Yan, Y. (2015). Vulnerability assessment and mitigation for the Chinese railway system under floods. Reliability Engineering & System Safety, 137, 58-68.

Iovine, G., D'Ambrosio, D., Di Gregorio, S. (2005). Applying genetic algorithms for calibrating a hexagonal cellular automata model for the simulation of debris flows characterised by strong inertial effects. Geomorphology, 66(1-4), 287-303.

Iverson, R. M., Schilling, S. P., Vallance, J. W (1998). Objective delineation of lahar-inundation hazard zones. Geological Society of America Bulletin, 110(8), 972-984.

Jaroszweski, D., Chapman, L., Petts, J. (2010). Assessing the potential impact of climate change on transportation: the need for an interdisciplinary approach. Journal of Transport Geography, 18, 331-335.

Johansson, I. (Ed.): Nordic Glossary of Hydrology, Almqvist and Wiksell International: Stockholm, 1984.

Kellermann, P., Schöbel, A., Kundela, G., and Thieken, A. H. (2015). Estimating flood damage to railway infrastructure – the case study of the March River flood in 2006 at the Austrian Northern Railway, Nat. Hazards Earth Syst. Sci., 15, 2485–2496

Kellermann, P., Schönberger, C., Thieken, A.H. (2016). Large-scale application of the flood damage model Railway Infrastructure Loss (RAIL). Nat. Hazards Earth Syst. Sci., 16, 2357–2371.

Koks, E. E., Rozenberg, J., Zorn, C., Tariverdi, M., Vousdoukas, M., Fraser, S. A., ... & Hallegatte, S. (2019). A global multi-hazard risk analysis of road and railway infrastructure assets. Nature communications, 10(1), 1-11. doi: https://doi.org/10.1038/s41467-019-10442-3

Lamb, R., Garside, P., Pant, R., & Hall, J. W. (2019). A probabilistic model of the economic risk to Britain's railway network from bridge scour during floods. Risk Analysis, 39(11), 2457-2478.

Lavers, D. A., Allan, R. P., Villarini, G., Lloyd-Hughes, B., Brayshaw, D. J., & Wade, A. J. (2013). Future changes in atmospheric rivers and their implications for winter flooding in Britain. Environmental Research Letters, 8(3), 034010.

Liu, X., Huang, Y., Xu, X., Li, X., Li, X., Ciais, P., ... & Zeng, Z. (2020). High-spatiotemporal-resolution mapping of global urban change from 1985 to 2015. Nature Sustainability, 3(7), 564-570.

Manfreda, S., Samela, C., Gioia, A., Consoli, G., Iacobellis, V., Giuzio, L., Cantisani, A., & Sole, A. (2015). Flood-Prone Areas Assessment Using Linear Binary Classifiers based on flood maps obtained from 1D and 2D hydraulic models. Natural Hazards, 79(2), 735-754.

Manfreda, S., & Samela, C. (2019). A digital elevation model based method for a rapid estimation of flood inundation depth. Journal of Flood Risk Management, 12, e12541; https://doi.org/10.1111/jfr3.12541.

Miller, D. J., Burnett, K. M. (2008). A probabilistic model of debris-flow delivery to stream channels, demonstrated for the Coast Range of Oregon, USA. Geomorphology, 94(1-2), 184-205.

Montgomery, D. R., Dietrich, W. E. (1994). A physically based model for the topographic control on shallow landsliding. Water Resources Research, 30(4), 1153-1171.

Montgomery, D. R., Foufoula-Georgiou, E. (1993). Channel network source representation using digital elevation models. Water Resources Research, 29(12), 3925-3934.

Moran, A. P., Thieken, A. H., Schöbel, A., and Rachoy, C. (2010). Documentation of Flood Damage on Railway Infrastructure, in: Data and Mobility, edited by: Düh, J., Hufnagl, H., Juritsch, E., Pfliegl, R., Schimany, H.-K., and Schönegger, H., AISC 81, Heidelberg, 61–70.

Nester, T., Schöbel, A., Drabek, U., Kirnbauer, R., and Rachoy, C. (2008). Flood Warning System for the Austrian Railways, in: 1st Lakeside Conference on Safety in Mobility, Intelligent, Weather Information Systems and Services in Traffic and Transport, Velden, Austria.

O'brien, J. S., Julien, P. Y., Fullerton, W. T. (1993). Two-dimensional water flood and mudflow simulation. Journal of hydraulic engineering, 119(2), 244-261.

Otto, A., Kellermann, P., Thieken, A.H., Costa, M.M., Carmona, M., Bubeck, P. (2019). Risk reduction partnerships in railway transport infrastructure in an alpine environment. International Journal of Disaster Risk Reduction, 33, 385-397.

Pastorello, R., Michelini, T., d'Agostino, V. (2017). On the criteria to create a susceptibility map to debris flow at a regional scale using Flow-R. Journal of Mountain Science, 14(4), 621-635.

Perez-Morales P., Gomariz-Castillo, F.,Pardo-Zaragoza, P. (2019). Vulnerability of Transport Networks to Multi-Scenario Flooding and Optimum Location of Emergency Management Centers. Water, 11, 1-19.

Petrova, E., & Bostenaru Dan, M. (2020). Preface: Natural hazard impacts on technological systems and infrastructures. Natural Hazards and Earth System Sciences, 20(10), 2627-2631.

Pirulli, M., Mangeney, A. (2008). Results of back-analysis of the propagation of rock avalanches as a function of the assumed rheology. Rock Mechanics and Rock Engineering, 41(1), 59-84.

Pregnolato, M., Ford, A., Wilkinson, S.M., Dawson, R.J. (2017). The impact of flooding on road transport: A depth-disruption function, Transportation Research Part D, 55, 67-81.

Prudhomme, C., & Genevier, M. (2011). Can atmospheric circulation be linked to flooding in Europe?. Hydrological processes, 25(7), 1180-1190.

Rickenmann, D. (2005). Runout prediction methods. In Debris-flow hazards and related phenomena (pp. 305-324). Springer, Berlin, Heidelberg.

Rickenmann, D., Zimmermann, M. (1993). The 1987 debris flows in Switzerland: documentation and analysis. Geomorphology, 8(2-3), 175-189.

Samela, C., Albano, R., Sole, A., Manfreda, S. (2018). A GIS tool for cost-effective delineation of flood-prone areas. Computers, Environment and Urban Systems, 70, 43-52.

Samela, C., Troy, T. J., Manfreda, S. (2017). Geomorphic classifiers for flood-prone areas delineation for data-scarce environments. Advances in water resources, 102, 13-28.

Santos, R., Duarte, R. M. (2006). Topographic signature of debris flow dominated channels: implications for hazard assessment. WIT Transactions on Ecology and the Environment, 90.

Singh, P., Sinha, V. S. P., Vijhani, A., & Pahuja, N. (2018). Vulnerability assessment of urban road network from urban flood. International journal of disaster risk reduction, 28, 237-250.

Takahashi, T. (2007). Debris flow: mechanics, prediction and countermeasures. Taylor & Francis.

Tavares da Costa, R., Manfreda, S., Luzzi, V., Samela, C., Mazzoli, P., Castellarin, A., & Bagli, S. (2019). A web application for hydrogeomorphic flood hazard mapping. Environmental Modelling & Software, 118, 172-186. DOI: https://doi.org/10.1016/j.envsoft.2019.04.010

Tellman, B., Sullivan, J., Kuhn, C., Kettner, A., Doyle, C., Brakenridge, G., ... & Slayback, D. (2021). Satellite imaging reveals increased proportion of population exposed to floods. Nature 596, 80–86. https://doi.org/10.1038/s41586-021-03695-w

Trigila A., Iadanza C., Bussettini M., Lastoria B. (2018). Dissesto idrogeologico in Italia: pericolosità e indicatori di rischio. Edizione 2018. ISPRA, Rapporti 287/2018 (ISBN 978-88-448-0901-0)

Tsubaki, R., Bricker, J.D., Ichii, K., Kawahara, Y. (2016). Development of fragility curves for railway embankment and ballast scour due to overtopping flood flow, Nat. Hazards Earth Syst. Sci., 16, 2455–2472.

van Ginkel, K. C. H., Dottori, F., Alfieri, L., Feyen, L., and Koks, E. E. (2021). Flood risk assessment of the European road network, Nat. Hazards Earth Syst. Sci., 21, 1011–1027, https://doi.org/10.5194/nhess-21-1011-2021, 2021.

Van Westen, C. J., Van Asch, T. W., Soeters, R. (2006). Landslide hazard and risk zonation—why is it still so difficult? Bulletin of Engineering geology and the Environment, 65(2), 167-184.

WMO: International Glossary of Hydrology, WMO Report No. 385, Geneva, 1974.

Zhu, W., Liu, K., Wang, M., Ward, P. J., & Koks, E. E. (2021). System vulnerability and risk assessment of railway systems to flooding. Natural Hazards and Earth System Sciences Discussions, 1-48.